AJNR

Reduction of CSF Artifacts on FLAIR Images by Using Adiabatic Inversion Pulses

Joseph V. Hajnal, Angela Oatridge, Amy H. Herlihy and Graeme M. Bydder

AJNR Am J Neuroradiol 2001, 22 (2) 317-322
http://www.ajnr.org/content/22/2/317

AJNR Am J Neuroradiol 22:317–322, February 2001

Technical Note

Reduction of CSF Artifacts on FLAIR Images by Using Adiabatic Inversion Pulses

Joseph V. Hajnal, Angela Oatridge, Amy H. Herlihy, and Graeme M. Bydder

Summary: The purpose of this study was to investigate the possibility that some artifactual high signals produced in CSF with fluid-attenuated inversion-recovery MR sequences could be due to inhomogeneity in the amplitude of the initial inversion pulse, and that this problem could be reduced or eliminated by the use of adiabatic inversion pulses. Studies with four volunteers showed dependence of high CSF signals in the posterior fossa on radiofrequency pulse amplitudes and that these signals could be eliminated by the use of adiabatic inversion pulses. Two illustrative clinical cases are included.

Although the fluid-attenuated inversion-recovery (FLAIR) pulse sequence is widely used, problems arise in the diagnosis of diseases of the brain and meninges because of spurious high signals in CSF (1–3). These signals may be due to pulsatile flow of CSF causing inflow of noninverted or only partially inverted CSF into the slice between the initial 180° pulse and the subsequent 90° pulse (4) as well as shortening of the T1 of CSF due to the presence of increased protein or molecular O_2 from inhalation of 100% O_2.

In this report we consider another potential cause of these signals; namely, inhomogeneity of the amplitude of the initial inversion pulse of FLAIR sequences. In parts of the body remote from the center of the transmitter coil, the amplitude of the radiofrequency (RF) field of an inversion pulse may be reduced such that the magnetization of tissues and fluids in these regions is only partly inverted. In brain imaging this is most likely to occur near the entrance to a typical bird cage transmit-receive head coil and may therefore affect mainly the posterior fossa and craniovertebral junction. In spine imaging, it is likely to be most apparent at the periphery of large fields of view (FOVs).

We performed simulations of this effect in imaging studies of four volunteers. We also compared the performance of FLAIR sequences in which conventional and adiabatic pulses were used to invert the initial magnetization, since adiabatic inversion pulses (5) provide full inversion over a wider range of RF amplitudes and would therefore be expected to reduce this effect. For comparison, similar studies were performed with short-inversion-time inversion-recovery (STIR) sequences. The STIR sequence is technically similar to the FLAIR sequence, but the consequences of an inadequate initial inversion pulse are quite different.

Received June 12, 2000; accepted after revision July 28.

From the Robert Steiner Magnetic Resonance Unit, MRC Clinical Sciences Centre, Imperial College School of Medicine, Hammersmith Campus, Du Cane Rd, London W12 0HS, UK.

Address reprint requests to G. M. Bydder.

Theory

The mode of operation of FLAIR and STIR sequences is illustrated in Figure 1. Calculated normalized signal strengths for these sequences are plotted as functions of RF flip angle for initial inversion pulses of different amplitudes in Figure 2. In each case, representative values of T1 and T2 have been used for the fluids or tissues concerned. TR was set at infinity and inversion time (TI) was chosen to null the appropriate fluid or tissue with a full inversion (ie, a flip angle of 180°, right-hand end of graphs). With incomplete inversion there is a failure to null the target tissue or fluid.

With the FLAIR sequence, incomplete inversion results in a failure of CSF suppression and a slight increase in signal from the brain (Fig 2A). With the STIR sequence, incomplete inversion produces an initial loss of the magnitude of the muscle signal and an increase in fat signal. This is followed by an artifactual reversal of contrast with fat having a higher signal than muscle. At a later stage, muscle has a higher signal than fat (Fig 2B).

The adverse effects of variations in local B_1 amplitude (or effective RF pulse flip angle) on the performance of inversion pulses may be mitigated by the use of adiabatic inversion pulses (5), which are more tolerant of variations in RF field amplitude. In adiabatic inversion pulses, the effective B_1 field rotates slowly from being parallel with B_0 to being antiparallel with B_0, and the magnetization follows it around. Providing the amplitude of the adiabatic pulses is above a threshold value, the magnetization is locked to B_1 so that proper inversion is assured.

Adiabatic pulses are not widely used for clinical imaging at the present time, but have been used (in nonselective form) with whole-body systems (6) and in conjunction with surface coil transmit systems (7–9). They have also been incorporated into inversion-recovery (IR) sequences for T1 measurements in spatially inhomogeneous B_1 fields (10, 11) and have been used with multiple inversion pulses to suppress background signal in MR angiography (12). A magnetization-prepared rapid acquisition gradient-echo version of the FLAIR sequence that incorporates adiabatic pulses has been described by Epstein et al (13).

Methods

All studies were performed on a 1.0-T MR system. In vivo tests were performed on four male volunteers (ages 38 to 65 years) who had given informed consent.

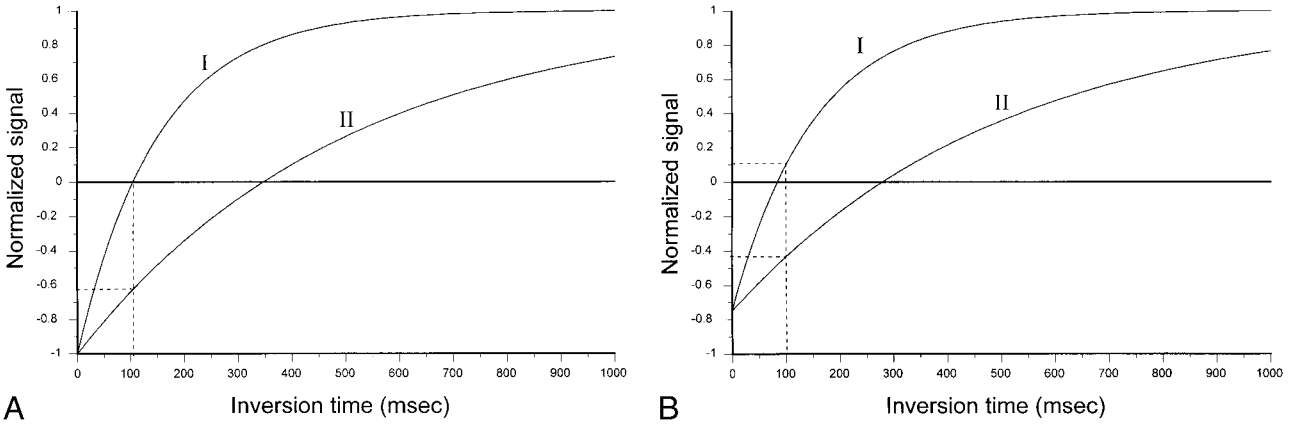

FIG 1. Operation of signal-nulling IR sequences. Normalized signal plotted against inversion time.

A, The longitudinal magnetization of the target tissue to be nulled must pass through zero when the 90° pulse is applied (*curve I*). Tissues with other T1 values (eg, *curve II*) produce signals at this time. For example, at 100 ms (when *curve I* passes through zero), *curve II* yields a signal of −0.63.

B, An incorrect flip angle of the inverting pulse produces only partial inversion of the longitudinal magnetization and now results in a recovery curve that has already passed through zero when the 90° pulse is applied (*curve I*) so that the target tissue is no longer nulled. The signal from the other tissue at this time is changed from −0.63 to −0.43.

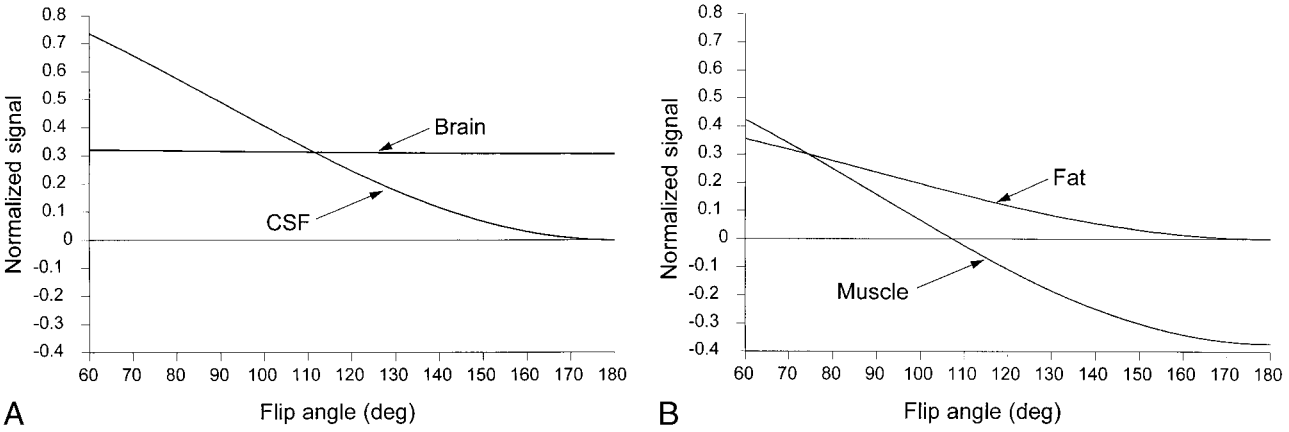

FIG 2. *A* and *B,* Signals (normalized to value at full relaxation) for FLAIR (*A*) and STIR (*B*) sequences plotted against RF flip angle (degrees) of the initial "inversion" pulse. Sequence parameters have been set at ∞/90 (TR/TE) and TI = 2100 for the FLAIR sequence and ∞/30, TI = 130 for the STIR sequence. 1.0-T values for tissue T1/T2 (ms) were used as follows: brain (mixed gray and white matter) = 700/80, CSF = 4500/4500, fat = 185/80, and muscle = 500/40. The desired performance (which is an effective flip angle of 180°) is shown at the extreme right-hand end of the graphs. For brain and CSF with the FLAIR sequence, there is a gradual rise of CSF signal as the flip angle is decreased (ie, shifts to the left). Equal signals are seen at 112°. With the STIR sequence, fat increases its signal as the flip angle is reduced. Muscle shows a reduced signal magnitude and is nulled at a flip angle of 108°. It has a higher signal than fat at flip angles less than 75° (*B*).

The initial inversion pulse of the conventional FLAIR sequence consisted of a 4-ms numerically optimized sinc pulse of bandwidth 557 Hz. For the adiabatic version of the FLAIR sequence, a phase-modulated hyperbolic secant adiabatic pulse (9) was implemented. Two adiabatic pulses were used, each with a peak RF amplitude of 23.5 μT. They were of 10- and 20-ms duration, with bandwidths (full width at half maximum) of 1554 and 777 Hz, respectively. Experiments on phantoms were performed to check the properties of both the conventional and adiabatic pulses. In these tests, the amplitude of the pulses was varied in equal increments from 0 to peak. The pulses under test were immediately followed by spoiler gradients (10 mT/m for 9 ms on all three axes). A standard spin-echo sequence with constant RF pulse amplitudes was then used to excite and measure the remaining longitudinal magnetization.

For the purposes of this study, conventional and adiabatic versions of the FLAIR pulse sequences were constructed with the same imaging parameters (apart from the initial inversion pulses described above). Interleaved FLAIR sequences were used. Ten 7-mm-thick slices with an imaging matrix of 128 × 256 were obtained for all in vivo studies. Imaging parameters for the FLAIR sequence were 6500/90/1 (TR/TE/excitations), TI = 2100, and FOV = 25 cm. FLAIR imaging was performed in the transmit-receive bird cage head coil. For the STIR sequences, imaging parameters were 2500/30/2, TI = 130, matrix = 128 × 256, slice thickness = 7 mm (10 slices), and FOV = 45 to 55 cm. STIR imaging was performed in the transmit-receive body coil. All the IR sequences were tested on phantoms to confirm their properties.

Test of Effects Attributable to RF Inhomogeneity in Volunteers

To test the basic hypothesis that artifactual failure to null selected signals with conventional FLAIR sequences could be due to RF inhomogeneity, we performed the following experiment. With subjects positioned such that the inferior aspect of

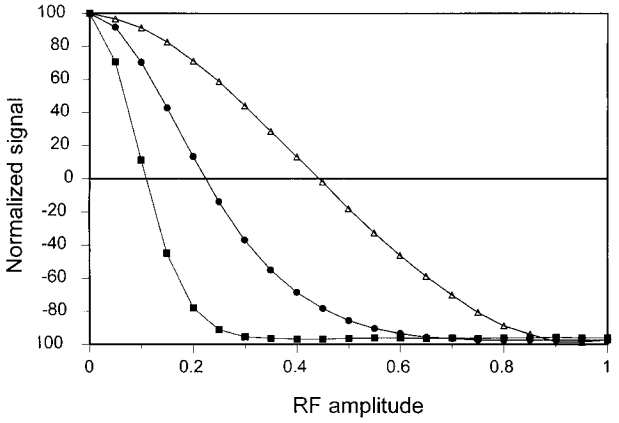

FIG 3. Graph of the normalized signal obtained after magnetization inversion followed by a 90° pulse plotted against RF amplitude for the conventional inversion pulse (*triangles*), the 10-ms adiabatic pulse (*circles*), and the 20-ms adiabatic pulse (*squares*). The adiabatic pulses provide full inversion over wider ranges of RF amplitudes (or effective flip angles) than does the conventional pulse.

the jaw was slightly outside the transmit-receive coil, conventional FLAIR images were acquired in the transverse plane. A slice-selective excitation located at a slice position that showed poor CSF suppression was then used to recalibrate the inversion pulse to a level designed to suppress the CSF signal in this region, and a further conventional FLAIR image was acquired.

Comparison of Conventional and Adiabatic Forms of the FLAIR Sequence in Volunteers

Comparative brain studies with conventional and adiabatic versions of the FLAIR sequence were also obtained in the four volunteers with the head positioned normally. In two volunteers, comparative studies of the lumbar spine and pelvis were obtained with conventional and adiabatic STIR sequences.

Signal suppression and signal-to-noise ratio (SNR) were assessed visually and by region-of-interest (ROI) measurements. The ROI data were used to calculate the SNR, which was defined as signal in nonsuppressed tissue divided by the standard deviation of noise in regions outside the body.

Results

Plots of normalized signal performance against RF amplitude for a conventional pulse and for the adiabatic inversion pulses are shown in Figure 3. Full inversion was achieved over a range of 90% to 100% of RF amplitude with the conventional pulse. Full inversion was achieved from 70% to 100% and from 35% to 100% of full amplitude for the 10- and 20-ms adiabatic pulses, respectively. The adiabatic pulses provided full inversion over a much wider range of RF amplitudes than did the conventional pulse.

Test of Effects Attributable to RF Inhomogeneity in Volunteers

The in vivo tests of conventional FLAIR sequences obtained from the healthy volunteers showed failure to suppress the CSF signal at the periphery of the transmitter field. Recalibration of the transmitter system to produce a higher-amplitude RF pulse resulted in suppression of the CSF signal at the specified peripheral location but a loss of CSF signal suppression in the images obtained from the central region of the coil. This experiment confirmed that the failure to suppress the CSF signal at the periphery of the coil was due to RF inhomogeneity, and could be rectified.

Comparison of Conventional and Adiabatic Versions of the FLAIR Sequence in Volunteers

Typical results of the comparative studies are illustrated in Figure 4, which shows conventional and adiabatic FLAIR sequences of the brain in a healthy volunteer. Performance of the two sequences was similar at the thalamic level (Fig 4A and B) but at the level of the pons there was a high signal in the CSF anterior to the pons and cerebellum when the conventional sequence was used (Fig 4C). The 10-ms adiabatic pulse increased the region of suppression in comparison with the conventional pulse. The 20-ms adiabatic variant increased the region of suppression further, and produced a low signal from CSF anterior to the pons and cerebellum (Fig 4D).

The SNR of white and gray matter was not affected by the use of adiabatic pulses, with values of 102, 100, and 101 for FLAIR sequences with conventional, 10-ms adiabatic, and 20-ms adiabatic pulses, respectively. The adiabatic FLAIR sequences tended to produce higher signals from inflowing blood than did the conventional version.

The STIR sequence showed the expected fat suppression over the central region of the FOV (Fig 5A). However, toward the periphery of the FOV (ie, in the retroperitoneum, superiorly, and at the level of the mid-shaft of the femur and below, inferiorly), fat signals abruptly increased and the muscle signal rapidly decreased. In addition, superiorly in the lumbar spinal canal, the CSF was of low signal (Fig 5A). The 10-ms adiabatic pulse reduced the magnitude of these effects and moved them farther peripherally. The 20-ms adiabatic version showed none of these problems and displayed appropriate tissue contrast over the full FOV, including no signal from fat, consistent signal from muscle, and high signal from CSF (Fig 5B). The signal from muscle is lower in Figure 5B because of T2 relaxation during the extended adiabatic (20-ms) pulse. There is a compromise between increasing tolerance to inhomogeneity of B_1 by using longer adiabatic pulses and loss of SNR due to T2 relaxation effects.

In the central part of the images, the SNR of muscle was 39 for the conventional sequence, 42 for the 10-ms adiabatic version, and 27 for the 20-ms adiabatic version. The SNR for regions of appropriate fat suppression was 3.4, 4.7, and 4.0 for the conventional, 10-ms, and 20-ms adiabatic pulse sequences, respectively.

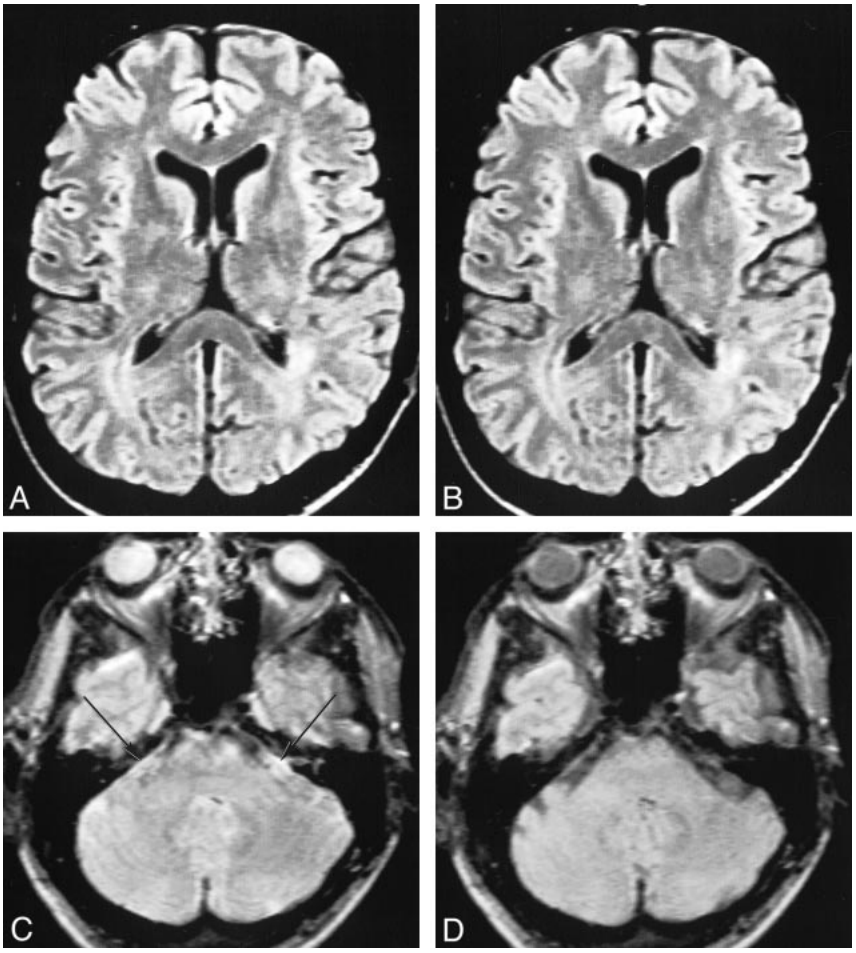

FIG 4. *A–D,* Comparison of FLAIR images of the brain in a healthy male volunteer aged 53 years. At the thalamic level, transverse slices show comparable CSF suppression and SNR for the conventional (*A*) and 20-ms adiabatic (*B*) pulse versions. At the level of the pons, the conventional sequence fails to suppress CSF anterior to the pons and cerebellum (*C, arrows*), whereas the 20-ms adiabatic version provides good CSF suppression (*D*).

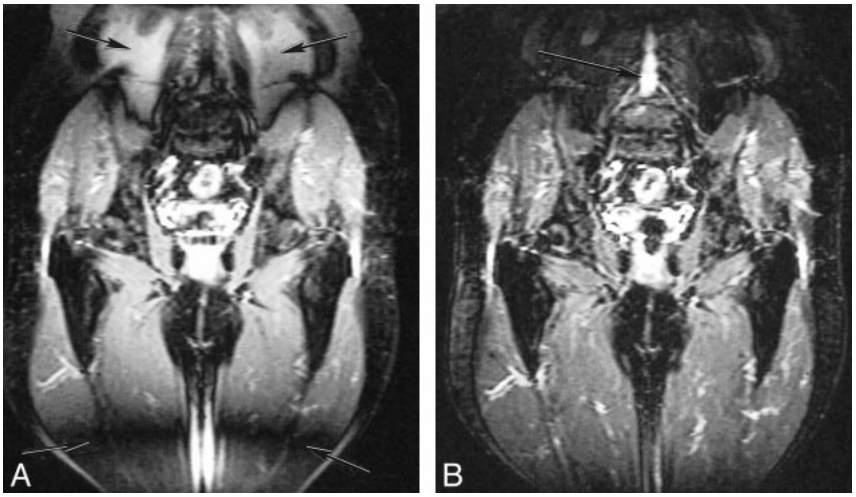

FIG 5. Comparison of coronal STIR sequences acquired through the lumbar spine and pelvis of a healthy male aged 65 years.

A, The conventional version only produces effective fat suppression in the central part of the image. Superiorly, fat has a high signal (*upper arrows*). CSF in this region has a low signal. The conventional sequence suppresses muscle at the level of the mid-shaft of the femur (*lower arrows*) and fat has a high signal inferior to this.

B, The 20-ms adiabatic version produces effective fat suppression and appropriate signals from muscle over the full FOV. CSF also has its normal high signal (*arrow*).

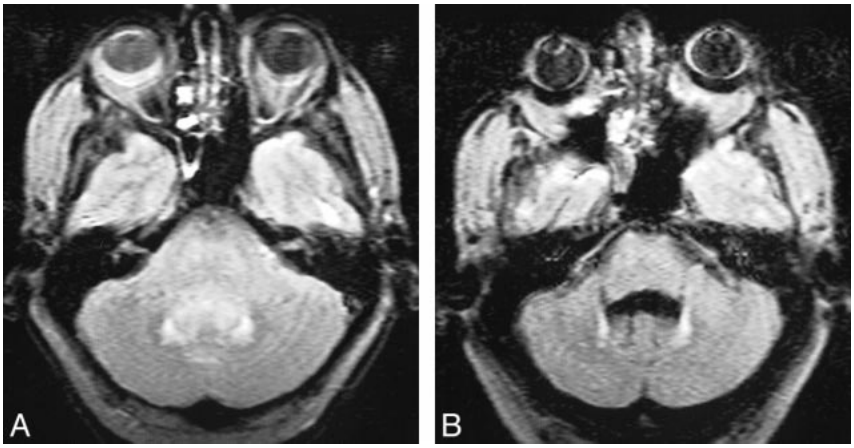

FIG 6. Hydrocephalus with edema around the fourth ventricle in a patient with a high-grade glioma.
A and *B,* Sinc (*A*) and 10-ms adiabatic (*B*) FLAIR sequences (8142/135, TI = 2200). CSF signal is markedly reduced in *B.*

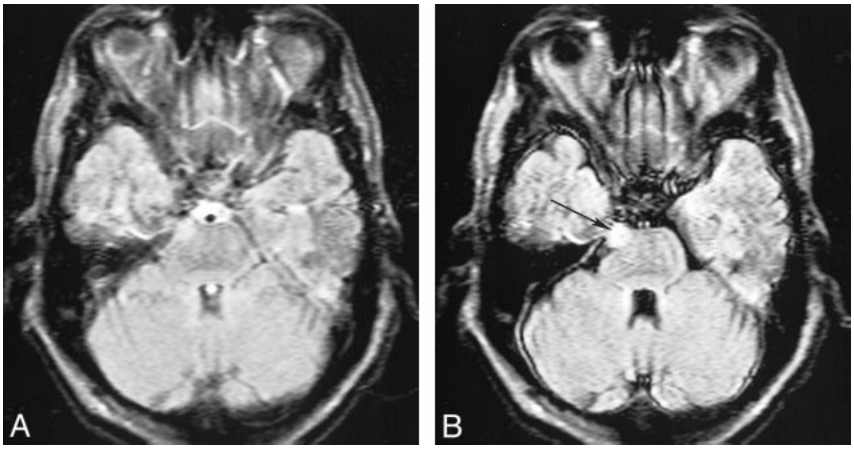

FIG 7. Patient with probable meningioma.
A and *B,* Sinc (*A*) and 10-ms adiabatic (*B*) FLAIR sequences (8142/135, TI = 2200). The tumor is more readily seen in *B* (*arrow*), without the high signal from CSF seen in *A.*

Clinical use of the technique is illustrated by comparing two FLAIR images obtained with a sinc pulse (Fig 6A) and a 10-ms adiabatic pulse (Fig 6B) in a 41-year-old man with an obstructive hydrocephalus and an enlarged fourth ventricle with associated edema. The brain stem and fourth ventricle are better seen in Figure 6B. Figure 7 shows sinc (Fig 7A) and 10-ms adiabatic (Fig 7B) FLAIR images in a 61-year-old man with a probable meningioma adjacent to the pons on the right. It is more readily seen in Figure 7B, where the CSF signal is more adequately suppressed.

Discussion

It is likely that each of the three mechanisms mentioned in the introduction (ie, inadequate initial inversion pulse, inflow of noninverted CSF, and reduction in the T1 of CSF) may play a role in the production of spurious high signals in CSF with FLAIR sequences. The effects of an inadequate initial inversion pulse may be ameliorated with an adiabatic inversion pulse, as described in this report. Effects caused by inflow of CSF may be reduced by widening the initial slice-selective inversion pulse (14) or by using 3D multislab methods (15). They may also be reduced by using a nonselective inversion pulse at the price of successively increasing values of TI for each slice (16) or by using a nonselective inversion pulse combined with k space reordered by inversion time at each slice position (KRISP) in the form of the KRISP-FLAIR sequence (17, 18). The effects of increased CSF protein in reducing CSF T1 can be compensated for by reducing the TI of the FLAIR sequence (19).

Comparison with the STIR sequence was of interest, because of its different mode of failure due to B_1 inhomogeneity. While failure of the FLAIR sequence produced a gradual increase in signal from CSF, which became higher than that of brain, failure of the STIR sequence produced a drastic loss of muscle signal and abrupt reversal of tissue contrast over a short distance, with the CSF signal becoming low rather than high. As a result, the problem is much easier to recognize with the STIR sequence than with the FLAIR sequence, in which

there may be no other sign of failure apart from a raised CSF signal. This insidious and frequently unpredictable change may cause diagnostic confusion, since it may also be the only sign produced by some disorders, such as subarachnoid hemorrhage.

One disadvantage of adiabatic pulses is their longer duration, which may account for the fact that they are not more widely used. This is likely to be a greater problem in sequences in which inversion pulses may be closely spaced than in the situation with the initial pulse of a FLAIR sequence. Adiabatic pulses are also often associated with a higher specific absorption rate than are conventional sequences. In spite of these difficulties we now use the adiabatic pulses for FLAIR imaging at conventional clinical field strengths.

References

1. Campbell BG, Comunale JP, Kelly LH, Zimmerman RD. **The subarachnoid space on fluid attenuated inversion recovery MR: all that is bright is not hemorrhage and all that is dark is not cerebrospinal fluid.** *Proceedings of the American Society of Neuroradiology, 36th Annual Meeting, May 17–21 1998.* Oak Book, IL: American Society of Neuroradiology; 1998:417
2. Yousem DM, Wu H. **Artifacts in the basal cisterns: the downfall of FLAIR.** *Radiology* 1999;213(P):145
3. Tubridy M, Barker GJ, MacManus DG, Mosely IF, Miller DH. **Optimization of unenhanced MRI for detection of lesions in multiple sclerosis: a comparison of five pulse sequences with variable slice thickness.** *Neuroradiology* 1998;40:293–297
4. Bakshi R, Caruthers SD, Janardhan V, Wasay M. **Intraventricular CSF pulsation artifact on fast fluid-attenuated inversion-recovery MR images: analysis of 100 consecutive normal studies.** *AJNR Am J Neuroradiol* 2000;21:503–508
5. Silver MS, Joseph RI, Hoult DI. **Highly selective $\pi/2$ and π pulse generation.** *J Magn Reson* 1984;59:347–351
6. Hutchison JMS, Edelstein WA, Johnson G. **A whole-body NMR imaging machine.** *J Phys E* 1980;136:947–955
7. Garwood M, Ugurbil K, Rath AR, et al. **Magnetic resonance imaging with adiabatic pulses using a single surface coil for RF transmission and signal detection.** *Magn Reson Med* 1989; 9:25–45
8. deGraaf RA, Nicolay K, Garwood M. **Single-shot, B1-insensitive slice selection with a gradient-modulated adiabatic pulse.** *Magn Reson Med* 1996;35:652–657
9. Van-Cauteren M, Miot F, Segebarth CM, Eisendrath H, Osteaux M, Willem R. **Excitation characteristics of adiabatic half-passage RF pulses used in surface coil MR spectroscopy: application to 13C detection of glycogen in the rat liver.** *Phys Med Biol* 1992;37:1055–1064
10. Hardy CJ, Edelstein WA, Vatis D, Harms R, Adams WJ. **Calculated T1 images derived from a partial saturation-inversion recovery pulse sequence with adiabatic fast passage.** *Magn Reson Imaging* 1985;31:107–116
11. Berkowitz BA, Wilson CA, Hatchell D, London SE. **Quantitative determination of the partial oxygen pressure in the vitrectomized rabbit eye *in vivo* using ^{19}F NMR.** *Magn Reson Med* 1991; 22:233–241, 512–513
12. Mani S, Pauly J, Conolly S, Meyer C, Nishimura D. **Background suppression with multiple inversion recovery nulling: applications to projective angiography.** *Magn Reson Med* 1997;37: 898–905
13. Epstein FH, Mugler JP III, Cail WS, Brookeman JR. **CSF-suppressed T2-weighted three-dimensional MP-RAGE MR imaging.** *J Magn Reson Imaging* 1995;4:463–469
14. De Coene B, Hajnal JV, Gatehouse P, et al. **MR of the brain using fluid attenuated inversion recovery (FLAIR) pulse sequences.** *AJNR Am J Neuroradiol* 1992;13:1555–1564
15. Barker GJ. **3D fast FLAIR: a CSF nulled 3D fast spin echo pulse sequence.** *Magn Reson Imaging* 1998;16:715–720
16. De Coene B, Hajnal JV, Pennock JM, Bydder GM. **MRI of the brain stem using fluid attenuated inversion recovery pulse sequences.** *Neuroradiology* 1993;35:327–331
17. Herlihy AH, Coutts GA, Larkman DJ, et al. **Use of k-space resolved FLAIR with a non-selective inversion pulse to reduce flow artifacts and provide uniform tissue contrast.** *Book of Abstracts, International Society of Magnetic Resonance in Medicine (ISMRM), Eighth Annual Meeting, Denver, Colorado, April 1–7, 2000.* Berkeley, CA: International Society of Magnetic Resonance in Medicine; 2000:1743
18. Herlihy AH, Oatridge A, Bydder GM, Hajnal JV. **K-space reordered by inversion-time at each slice position (KRISP) FLAIR: applications to the brain and spinal cord.** *International Society of Magnetic Resonance in Medicine (ISMRM), Sixth Annual Meeting of the British Chapter, Liverpool, June 26–27, 2000.* Berkeley, CA: International Society of Magnetic Resonance in Medicine; 2000:73
19. Essig M, Bock M. **Optimization of fluid-attenuated inversion recovery (FLAIR) MR imaging in patients with high CSF blood or protein content.** *Magn Reson Med* 2000;43:764–767